An In-Body Impulse Radio Transceiver with Implant Antenna Miniaturization at 30 MHz

Jianqing Wang, *Member, IEEE,* Jinlong Liu, Kohei Suguri, and Daisuke Anzai, *Member, IEEE*

***Abstract*—For real-time image/video transmission in implant body area networks, we have developed an in-body transceiver at around 30 MHz. The transceiver employs impulse radio (IR) technology with multi-pulse position modulation (MPPM) scheme. The transmit antenna was realized in a dimension of 1 $\times$ 2 cm by forming the radiation elements on a flexible magnetic sheet. Experimental results in a biological-equivalent liquid phantom have demonstrated a bit error rate smaller than 10^{-3} in a depth of 26 cm with a data rate at least 1.25 Mbps.**

***Index Terms*—Implant communication, impulse radio transceiver, implant antenna, bit error rate, body area network.**

I. Introduction

WIRELESS body area communication is attracting much attention in medical and health care applications [1]. One of typical applications is wireless electronic pills to deliver real time video image of small intestine. As summarized in [2], wireless electronic pills usually employ 400 MHz band. Due to the limitation of frequency regulation in this band and the adoption of narrow-band modulation schemes, the available data rates are at the order of several hundred kbps. In view of the applications of implant communications, a data rate as high as several Mbps should be required. To increase the data rate, ultra wide band (UWB) transmission in a living animal has been attempted in [3], which showed a possibility to secure a bit error rate (BER) of 10^{-2} at 1 Mbps in a depth of 5 cm. In addition, in [4] a data rate of 2.5 Mbps was achieved in air for a transceiver at 20 MHz band. But its performance in actual biological body is unclear.

Since the human body is a lossy dielectric medium, the wavelength is shortened due to the frequency-dependent tissue properties. As compared to a penetration depth of 5.3 cm at 400 MHz and 1.7 cm at 4.1 GHz in muscle tissue, the penetration depth is as large as 8 cm at 30 MHz. This frequency band can therefore provide a significant improvement on the transmission distance in the human body. This frequency band is known as the extremely weak radio band where the use of frequency band is free until 322 MHz as long as the radiated electric field intensity is lower than 500 μV/m at a distance of 3 m [5]. However, for an electronic pill, the transmitter should not exceed a dimension in 1-cm diameter and 2-cm length usually for being easy to swallow [2]. This makes the realization of a small-size transmit antenna a key point in this frequency band.

The authors are with Nagoya Institute of Technology, Nagoya 466-8555, Japan e-mail: (wang@nitech.ac.jp).

Manuscript received February 9, 2015; revised April 9, 2015. This study was supported in part by JSPS KAKENHI Grant Number 15H04006.

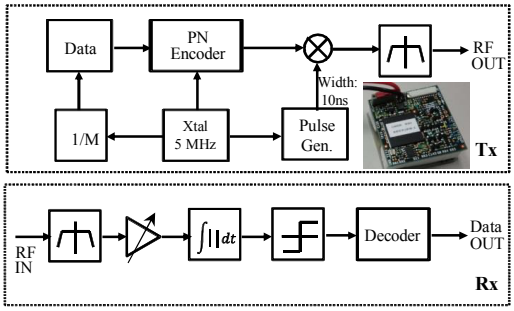

Fig. 1. Block diagram of the in-body IR transceiver.

In this study, we aim to develop an in-body transceiver at 30 MHz for reaching a high data rate above 1 Mbps. At first we design the implant transmit antenna for miniaturization. Then we evaluate the performances of antenna and transceiver with biological-equivalent liquid phantom to show the feasibility of the in-body high-speed transmission.

II. Transceiver Structure

In the 30 MHz band, impulse radio (IR) technique provides the possibility to realize a high data rate in the order of Mbps by directly transmitting short pulses based on digital bits [6]. Fig. 1 shows the block diagram of the developed in-body IR transceiver. The digitized image/video signals are modulated with short pulses based on IR scheme in the transmitter. The oscillator is used to produce clock signal at 5 MHz, and the pulse generator is used to produce pulses to be transmitted with a width of 10 ns. In order to transmit the digitized information bits, we first encode the digital bits ”0” and ”1” with two PN codes, and then use the pulses to represent chip ”1” and nothing for chip ”0”, which is actually a MPPM modulation. By adjusting the pulse number within one-bit period, the data rate can change from 1.25 Mbps (M = 4) to 5 Mbps (M = 1). The modulated pulses are spectrum-formed by the band pass filter (BPF) at the transmitter output as well as the band-pass features of the transmit and receive antennas.

On the other hand, the receiver employs an envelope detector for demodulation. The received signal is filtered and amplified, and is then adjusted to an adequate level by an automatic gain controller (AGC). After the envelope detector, the signal is judged as chip “0” or “1” by a comparator, and then decoded to reproduce the transmitted information bits. Table I summarizes the specifications of the developed IR transceiver. The in-body transceiver was assembled in a 3 cm $\times$ 3 cm printed circuit board, and has a power consumption of about 4.8 mW. Except for the crystal oscillator and the BPF, all the other parts such as the PN encoder, 1/M

TABLE I
IR TRANSCEIVER SPECIFICATIONS

Pulse width	10 ns
Pulse number per bit	8, 4, 2
Frequency band	10 - 60 MHz
Modulation	IR PPM
Data rate	1.25 Mbps, 2.5 Mbps, 5 Mbps
Maximum output	-15 dBm
Demodulation	Envelope detection
Clock recovery	Digital phase locked loop

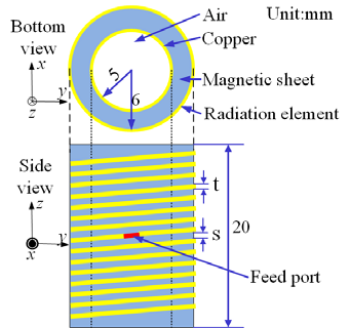

Fig. 2. Antenna structure.

divider, pulse generator and multiplier were realized with a commercially available field programmable gate array (FPGA, Xilinx Sparian-6). In view of that the BPF could also be realized as a digital filter, it is available to integrate all the parts in one chip with a smaller size for actual implant applications.

III. Antenna Structure

The implant transmit antenna needs a small size of 1-cm diameter and 2-cm length. However, the 30 MHz band signal has a wavelength λ_0 of 10 meters in free space. In order to shorten the wavelength for antenna miniaturization, we paid attention to flexible magnetic sheets. A magnetic sheet has both a high relative permittivity ε_r and a high relative permeability μ_r. So we can expect a double effect on shortening the wavelength by manufacturing the antenna radiation element on the magnetic sheet because the wavelength $\lambda \cong \lambda_0/\sqrt{\varepsilon_r \mu_r}$ in a magnetic material. The flexibility of the magnetic sheet also benefits to form a cylindrical pill shape. Fig. 2 shows the structure of the implant transmit antenna, which is actually a dipole structure with a reflection plane. The inner cylinder with a radius of a mm is composed of a copper-covered polyester cylinder. The polyester could sustain a sufficient weight without obvious deformation. The copper plane acts as the reflection plane of the antenna. The flexible magnetic sheet is covered on the copper-covered polyester cylinder with a thickness of 1 mm. The two dipole elements are two t-mm-thick copper wires. They are wrapped n turns over the magnetic sheet, respectively, with a spacing of s mm, and are further bonded with glue. Such a structure makes the antenna robust enough when inserting it into human tissues. The feeding point is at the center along the axis direction of the cylinder.

The antenna dimensions were determined by using an electromagnetic field simulation tool based on the finite element method (Ansys, HFSS) to determine the parameters a, t, s and n for a commercially available magnetic sheet with μ_r = 20.7, $\tan\delta_\mu$ = 0.12, ε_r = 13, and $\tan\delta_\varepsilon$ = 0.17, where $\tan\delta_\mu$ is the magnetic loss tangent and $\tan\delta_\epsilon$ is the dielectric loss tangent.

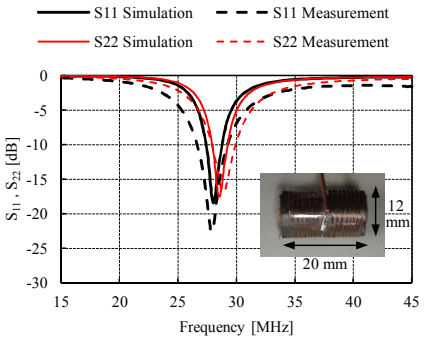

Fig. 3. Measured and simulated S_{11} and S_{22} as a function of frequency.

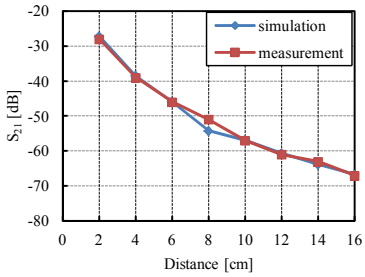

Fig. 4. Measured and simulated S_{21} as a function of distance at 30 MHz.

The antenna was inserted into a biological-equivalent liquid phantom with a dimension of 28 cm × 16 cm × 28 cm. The liquid phantom was made of deionized water, sugar, sodium chloride and so on, and its dielectric properties were adjusted to be ϵ_r = 56.05 and conductivity σ = 0.52 S/m at 30 MHz, nearly 2/3 times muscle's values. The S-parameter $S_{11} < -10$ dB was used as a target of the antenna design at 30 MHz. As a design result of numerical simulations, we determined the inner radius of the cylinder a = 5 mm, the thickness of the cooper wire t = 0.315 mm, the spacing between cooper wires s = 0.315 mm, and the number of turns n = 7. This design made the total length of the radiation element be 0.52 m, which is close to but somewhat longer than $\lambda/2$ in the magnetic material, because the outside of the copper wires are not magnetic material but air. For the receive antenna used on the body surface, we employed the same structure as the implant transmit antenna except that we increased the number of turns n to 7.5. Of course the receive antenna can be designed with larger dimensions for increasing its efficiency because it is on the body surface.

The S_{11}, S_{22} and S_{21} of the antennas were measured with a network analyzer and the biological-equivalent liquid phantom. The container of the liquid phantom was 2-mm thick plastic. No any change in the shape and structure was observed when inserting the antenna into the liquid phantom. Fig. 3 shows the measured S_{11} for the transmit antenna, wrapped in vinyl for insulation in the liquid phantom, and S_{22} for the receive antenna on the phantom surface, together with the simulated results for verification. It can be seen that both S_{11} and S_{22} have good agreement between the measurement and simulation. The slight difference beyond the central frequency of 30 MHz may be attributed to uncertainties of the electrical properties of the magnetic sheet used in the simulation. From the measured S_{11} and S_{22}, the antennas exhibited an absolute -10 dB bandwidth larger than 2.2 MHz.

Moreover, the transmission characteristic S_{21} was also measured when the transmit antenna and the receive antenna with a parallel arrangement. The transmit antenna was moved inside the phantom along a horizontal line to change the distance from the transmit antenna to the receive antenna. The receive antenna was fixed at the phantom surface with a spacing of 5 mm to the phantom. Fig. 4 shows the measured S_{21} at the central frequency of 30 MHz in comparison with the simulated one. Good agreement between them assures the validation of the designed and manufactured antennas. From the measured S_{21}, it is confirmed that the transmission loss is around 65 dB in a depth of 15 cm of the phantom. This transmission loss contains not only the path loss in the biological-equivalent liquid phantom but also the transmit and receive antenna gains, and is significantly smaller than that at 400 MHz or UWB band. This feature suggests a better communication performance for the developed antenna and transceiver.

IV. Communication Performance Evaluation

We then connected the transmit antenna to the transmitter and the receive antenna to the receiver for implant communication performance evaluation. Since the transmit and receive antennas have a narrower frequency band at 30 MHz, the IR signal is re-formed to have a narrow bandwidth. Fig. 5(a) shows the frequency spectrum of the transmitted pulse waveform at the output of transmitter before the transmit antenna, which exhibits a wide bandwidth ranging from 10 to 60 MHz. However, for the received pulse waveform at the input of receiver (after the receive antenna), due to the band-pass effect of the transmit and receive antennas, the received signal components are mainly around 30 MHz as shown in Fig. 5(b). Other frequency components are 15 dB smaller than that at the central frequency.

With the developed antenna/transceiver, we conducted the BER measurement for implant communication performance evaluation. The transmit antenna was inserted in the liquid phantom and connected to the transmitter in the outside of the phantom via a coaxial cable. Although the prototype transmitter was not directly implanted in the liquid phantom due to its insufficiency of waterproof function, the measurement setup should be effective in simulating an implant communication because possible radiation from the coaxial cable between the implant antenna and the transmitter was removed by attaching a number of ferrite cores. The receive antenna and receiver were set at the phantom surface with a 5-mm spacing. The receiver was connected to a personal computer via USB cable for data recording and BER counting. Fig. 6 shows the measured BER performance as a function of distance from the implant antenna to the phantom surface. As a result, up to a depth of 26 cm inside the liquid phantom, the BER smaller than 10^{-3} was obtained in the physical layer. The flat BER performance is attributed to the AGC in the receiver front-end. The received signal power attenuated according to the communication distance, but the AGC amplified the signal to a constant level or a constant power. The noise power at the front-end was also amplified simultaneously. This resulted in an almost constant SNR, and then a flat BER performance. As for the non-zero BER even at a short distance, it should

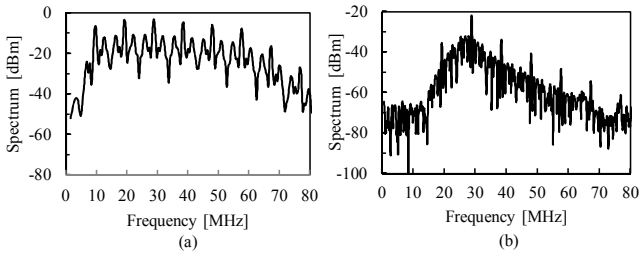

Fig. 5. (a) Spectrum of transmitted pulse at the output of transmitter, (b) spectrum of received pulse at the input of receiver.

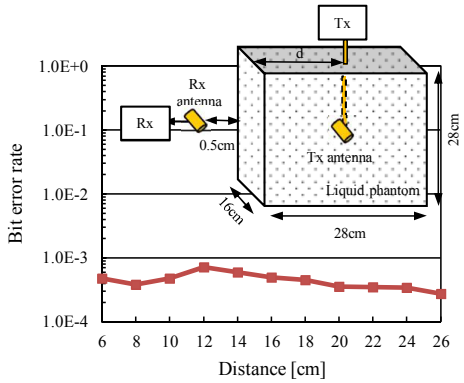

Fig. 6. Measured BER as a function of distance.

be due to a timing error in the phase-locked-loop clock recovery circuit, which needs further improvement. It is clear that the developed transceiver has achieved a reliable implant communication distance of at least 26 cm at a data rate of at least 1.25 Mbps, which provides a higher transmission speed and a deeper communication distance, compared to currently reported implant communication techniques in [2].

V. Conclusion

Real-time image/video transmission requires a high data rate at Mbps in wireless implant communications. For this purpose, we have developed an in-body IR transceivers with a small-size implant antenna at 30 MHz. The miniaturization of the antenna has been realized by forming the antenna radiation elements over a flexible magnetic sheet based on its double shortening effect of wavelength. The measurement results in a biological-equivalent liquid phantom have demonstrated a BER smaller than 10^{-3} in the physical layer in a depth of at least 26 cm with a date rate of at least 1.25 Mbps. This performance sufficiently shows the feasibility and usefulness of our developed in-body transceiver for high-speed implant communication in electronic pill applications.

References

[1] J. Wang and Q. Wang, *Body Area Communications*, Wiley-IEEE, 2013.
[2] M.R. Yuce, and T. Dissanayake, "Easy-to-swallow wireless telemetry," IEEE Microwave Magazine., vol. 13, no. 6, pp. 90-101, Sept. 2012.
[3] S. Itoh, S. Kawahito, and S. Terakawa, "A 2.6mW 2fps QVGA CMOS one-chip wireless camera with digital image transmission function for capsule endoscopes," in Proc. Int. Symp. on Circuits & Systems, Kos, Greece, pp. 3353-3356, 2006.
[4] D. Anzai, K. Katsu, R. Chavez-Santiago, Q. Wang, D. Plettemeier, J. Wang and I. Balasingham, "Experimental evaluation of implant UWB-IR transmission with living animal for body area networks," IEEE Trans. Microwave Theory Tech., vol.62, no.1, pp.183-192, Jan. 2014.
[5] Online: http://www.tele.soumu.go.jp/e/index.htm
[6] K. Shikada and J. Wang, "Development of human body communication transceiver based on impulse radio scheme," Proc. IEEE CPMT Symp. Japan, Kyoto, pp.283-286, Dec. 2012.